JOURNAL OF Applied Polymer SCIENCE

Special Issue: Microfiltration and Ultrafiltration Membrane Science and Technology

Guest Editors: Prof. Isabel C. Escobar (University of Toledo) and Prof. Bart Van der Bruggen (University of Leuven)

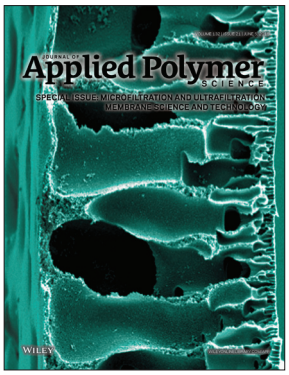

EDITORIAL

Microfiltration and Ultrafiltration Membrane Science and Technology
I. C. Escobar and B. Van der Bruggen, *J. Appl. Polym. Sci.* 2015, **DOI: 10.1002/app.42002**

REVIEWS

Nanoporous membranes generated from self-assembled block polymer precursors: *Quo Vadis*?
Y. Zhang, J. L. Sargent, B. W. Boudouris and W. A. Phillip, *J. Appl. Polym. Sci.* 2015, **DOI: 10.1002/app.41683**

Making polymeric membranes anti-fouling via "grafting from" polymerization of zwitterions
Q. Li, J. Imbrogno, G. Belfort and X.-L. Wang, *J. Appl. Polym. Sci.* 2015, **DOI: 10.1002/app.41781**

Fouling control on MF/ UF membranes: Effect of morphology, hydrophilicity and charge
R. Kumar and A. F. Ismail, *J. Appl. Polym. Sci.* 2015, **DOI: 10.1002/app.42042**

EMERGING MATERIALS AND FABRICATION

Preparation of a poly(phthalazine ether sulfone ketone) membrane with propanedioic acid as an additive and the prediction of its structure
P. Qin, A. Liu and C. Chen, *J. Appl. Polym. Sci.* 2015, **DOI: 10.1002/app.41621**

Preparation and characterization of MOF-PES ultrafiltration membranes
L. Zhai, G. Li, Y. Xu, M. Xiao, S. Wang and Y. Meng, *J. Appl. Polym. Sci.* 2015, **DOI: 10.1002/app.41663**

Tailoring of structures and permeation properties of asymmetric nanocomposite cellulose acetate/silver membranes
A. S. Figueiredo, M. G. Sánchez-Loredo, A. Maurício, M. F. C. Pereira, M. Minhalma and M. N. de Pinho, *J. Appl. Polym. Sci.* 2015, **DOI: 10.1002/app.41796**

LOW-FOULING POLYMERS

Low fouling polysulfone ultrafiltration membrane via click chemistry
Y. Xie, R. Tayouo and S. P. Nunes, *J. Appl. Polym. Sci.* 2015, **DOI: 10.1002/app.41549**

Elucidating membrane surface properties for preventing fouling of bioreactor membranes by surfactin
N. Behary, D. Lecouturier, A. Perwuelz and P. Dhulster, *J. Appl. Polym. Sci.* 2015, **DOI: 10.1002/app.41622**

PVC and PES-*g*-PEGMA blend membranes with improved ultrafiltration performance and fouling resistance
S. Jiang, J. Wang, J. Wu and Y. Chen, *J. Appl. Polym. Sci.* 2015, **DOI: 10.1002/app.41726**

Improved antifouling properties of TiO_2/PVDF nanocomposite membranes in UV coupled ultrafiltration
M. T. Moghadam, G. Lesage, T. Mohammadi, J.-P. Mericq, J. Mendret, M. Heran, C. Faur, S. Brosillon, M. Hemmati and F. Naeimpoor, *J. Appl. Polym. Sci.* 2015, **DOI: 10.1002/app.41731**

Development of functionalized doped carbon nanotube/polysulfone nanofiltration membranes for fouling control
P. Xie, Y. Li and J. Qiu, *J. Appl. Polym. Sci.* 2015, **DOI: 10.1002/app.41835**

JOURNAL OF Applied Polymer SCIENCE

Special Issue: Microfiltration and Ultrafiltration Membrane Science and Technology

Guest Editors: Prof. Isabel C. Escobar (University of Toledo) and
Prof. Bart Van der Bruggen (University of Leuven)

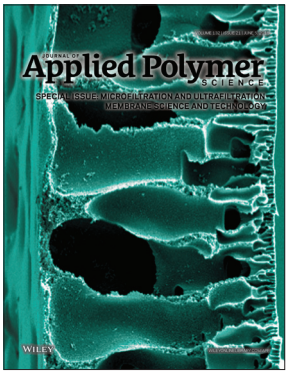

SURFACE MODIFICATION OF POLYMER MEMBRANES

Highly chlorine and oily fouling tolerant membrane surface modifications by *in situ* polymerization of dopamine and poly(ethylene glycol) diacrylate for water treatment
K. Yokwana, N. Gumbi, F. Adams, S. Mhlanga, E. Nxumalo and B. Mamba, *J. Appl. Polym. Sci.* 2015, **DOI: 10.1002/app.41661**

Fouling control through the hydrophilic surface modification of poly(vinylidene fluoride) membranes
H. Jang, D.-H. Song, I.-C. Kim, and Y.-N. Kwon, *J. Appl. Polym. Sci.* 2015, **DOI: 10.1002/app.41712**

Hydroxyl functionalized PVDF-TiO_2 ultrafiltration membrane and its antifouling properties
Y. H. Teow, A. A. Latif, J. K. Lim, H. P. Ngang, L. Y. Susan and B. S. Ooi, *J. Appl. Polym. Sci.* 2015, **DOI: 10.1002/app.41844**

Enhancing the antifouling properties of polysulfone ultrafiltration membranes by the grafting of poly(ethylene glycol) derivatives via surface amidation reactions
H. Yu, Y. Cao, G. Kang, Z. Liu, W. Kuang, J. Liu and M. Zhou, *J. Appl. Polym. Sci.* 2015, **DOI: 10.1002/app.41870**

SEPARATION APPLICATIONS

Experiment and simulation of the simultaneous removal of organic and inorganic contaminants by micellar enhanced ultrafiltration with mixed micelles
A. D. Vibhandik, S. Pawar and K. V. Marathe, *J. Appl. Polym. Sci.* 2015, **DOI: 10.1002/app.41435**

Polymeric membrane modification using SPEEK and bentonite for ultrafiltration of dairy wastewater
A. Pagidi, Y. Lukka Thuyavan, G. Arthanareeswaran, A. F. Ismail, J. Jaafar and D. Paul, *J. Appl. Polym. Sci.* 2015, **DOI: 10.1002/app.41651**

Forensic analysis of degraded polypropylene hollow fibers utilized in microfiltration
X. Lu, P. Shah, S. Maruf, S. Ortiz, T. Hoffard and J. Pellegrino, *J. Appl. Polym. Sci.* 2015, **DOI: 10.1002/app.41553**

A surface-renewal model for constant flux cross-flow microfiltration
S. Jiang and S. G. Chatterjee, *J. Appl. Polym. Sci.* 2015, **DOI: 10.1002/app.41778**

Ultrafiltration of aquatic humic substances through magnetically responsive polysulfone membranes
N. A. Azmi, Q. H. Ng and S. C. Low, *J. Appl. Polym. Sci.* 2015, **DOI: 10.1002/app.41874**

BIOSEPARATIONS APPLICATIONS

Analysis of the effects of electrostatic interactions on protein transport through zwitterionic ultrafiltration membranes using protein charge ladders
M. Hadidi and A. L. Zydney, *J. Appl. Polym. Sci.* 2015, **DOI: 10.1002/app.41540**

Modification of microfiltration membranes by hydrogel impregnation for pDNA purification
P. H. Castilho, T. R. Correia, M. T. Pessoa de Amorim, I. C. Escobar, J. A. Queiroz, I. J. Correia and A. M. Morão, *J. Appl. Polym. Sci.* 2015, **DOI: 10.1002/app.41610**

Hemodialysis membrane surface chemistry as a barrier to lipopolysaccharide transfer
B. Madsen, D. W. Britt, C.-H. Ho, M. Henrie, C. Ford, E. Stroup, B. Maltby, D. Olmstead and M. Andersen, *J. Appl. Polym. Sci.* 2015, **DOI: 10.1002/app.41550**

Membrane adsorbers comprising grafted glycopolymers for targeted lectin binding
H. C. S. Chenette and S. M. Husson, *J. Appl. Polym. Sci.* 2015, **DOI: 10.1002/app.41437**

Journal of Applied Polymer Science

Improved antifouling properties of TiO_2/PVDF nanocomposite membranes in UV-coupled ultrafiltration

Maryam Tavakol Moghadam,[1,2] Geoffroy Lesage,[2] Toraj Mohammadi,[1] Jean-Pierre Mericq,[2] Julie Mendret,[2] Marc Heran,[2] Catherine Faur,[2] Stephan Brosillon,[2] Mahmud Hemmati,[1] Freshteh Naeimpoor[1]

[1]Research Centre for Membrane Separation processes, Faculty of Chemical Engineering, University of Science and Technology, Narmak, 16846 Tehran, Iran

[2]Institut Européen des Membranes, CNRS, UMR 5635, Université Montpellier II, Montpellier, France

Correspondence to: M. T. Mohammadi (E-mail: torajmohammadi@iust.ac.ir)

ABSTRACT: A polyvinylidene fluoride (PVDF) ultrafiltration (UF) membrane was modified by dispersing titanium oxide (TiO_2) particles in a PVDF solution. PVDF flat-sheet membranes were prepared by a phase inversion method. This study investigates the potential low-fouling properties of these composite membranes during filtration, in darkness or under UV irradiation, of pure water and foulants representative of those found in membrane bioreactor processes: commercial bovine serum albumin (BSA) as a model protein and real soluble extracellular polymeric substances (EPS). The experimental results indicate that nanocomposite membrane has a structure with longer and larger macrovoid than neat PVDF membranes resulting in higher water flux performances. These higher flux performances were also due to an increase in surface hydrophilicity because of the presence of TiO_2 particles. Moreover, such membranes are less prone to adsorption by BSA and present self-cleaning ability under static irradiation. During filtration of BSA and EPS without UV irradiation, nanocomposite membranes presented a little flux decline and reached stabilization more rapidly in comparison with PVDF membranes. Moreover, simultaneous UV irradiation during ultrafiltration has a benefit effect only on nanocomposite membranes for which initial flux was increased. Hydrophilic properties of nanocomposite membranes lead to better retention performances of BSA and EPS, which are still improved under UV irradiation. Finally, nanocomposite membranes under UV irradiation presented the best flux recovery ratio confirming their antifouling property. © 2014 Wiley Periodicals, Inc. J. Appl. Polym. Sci. **2015**, *132*, 41731.

KEYWORDS: composites; membranes; properties and characterization; synthesis and processing

Received 28 July 2014; accepted 3 November 2014

DOI: 10.1002/app.41731

INTRODUCTION

Growing global demand for clean water and increasing stringent environmental regulations make membrane filtration, that is the technology of choice for many wastewater treatment applications. This is due to membrane benefits and special features such as compactness, and the ease of fabrications, operation, and module design.[1] However, membrane fouling, which leads to frequent cleaning of membranes causing momentarily stopping in filtration and shortening membrane life, is still one of the main challenges in any membrane process.[2] Selection of an appropriate membrane,[3] optimization of operating conditions and hydraulic and chemical cleaning,[2,4] are all known to effectively minimize or remove fouling. These techniques often increase the total operational cost of the membranes as well as shorten their life time. In addition to these techniques, surface modification of membranes so as to make them less prone to irreversible fouling has become a point of interest for both researchers and industry.[2,3,5,6] For example, surface modification of polyvinylidene fluoride (PVDF) membranes by incorporation of inorganic nanoparticles to make nanocomposite membranes has been proposed as an effective method to improve membranes hydrophilicity and antifouling properties.[3,7] Indeed, among various polymeric membrane materials suitable for wastewater treatment, PVDF has drawn much attention due to its outstanding mechanical and physicochemical properties besides good thermal and chemical resistance to acid and basis cleaning.[8] However, current applications suffer from low fouling resistance of PVDF membranes due to their intrinsic hydrophobic properties.[8,9] Among different nanoparticles, titanium dioxide (TiO_2) has received much attention because of its stability, availability, and promise for water treatment applications due to its potential antifouling abilities[10–12] and photocatalytic property.[9,13–15]

The incorporation of widely available commercial TiO_2 powders into polymeric membranes is thus one of the strategies to improve antifouling performance of the membranes. There are two main approaches for the fabrication of TiO_2 nanocomposite membranes: (1) blending the nanoparticles into the membrane and (2) depositing the nanoparticles onto the surface of the membrane. Compare to coating approach, blending has some advantages, such as simplicity, because the particles are added to the membrane casting solution directly. Moreover, nanoparticles entrapped in the membrane matrix are less prone to release in which limitation is an important challenge in the field of composite polymeric/nanoparticles membranes.

Many studies have investigated improvements of PVDF membrane performances by TiO_2 blending.[9,16–21] Damodar *et al.* prepared modified PVDF membranes by adding different amounts of TiO_2 particles into the casting solution and investigated their antibacterial, photocatalytic, and antifouling properties.[16] Results showed that TiO_2 addition significantly affected the pore size and hydrophilicity of the membrane and thus improved the flux and permeability of the modified PVDF/TiO_2 membrane. TiO_2-doped PVDF membrane also showed better bactericidal and antifouling abilities under UV light exposure compared with the neat PVDF membrane.

Song *et al.*[9] evaluated photocatalytic properties of TiO_2-doped PVDF membranes and showed that membrane fouled with natural organic matter could be cleaned within 30 min under irradiation due the TiO_2/PVDF good self-cleaning ability and the photocatalytic properties.

The antifouling ability of TiO_2-entrapped PVDF membranes under UV irradiation has been proved in many researches. However, in most previous researches, the effect of separate UV irradiation has been investigated, and there is little information on the effect of continuous UV irradiation during filtration. Moreover, few studies that investigated continuous irradiation similar to Song *et al.*[9] were not performed in fouling conditions representative of those occurring in a MBR.

In this way, the objective of this study is to investigate the antifouling properties of nanocomposite PVDF/TiO_2 membranes toward foulants encountered during filtration in MBR. In addition, influence of static and continuous UV irradiation on fouling removal was evaluated. TiO_2/PVDF composite membranes were prepared via phase inversion method by adding TiO_2 nanoparticles to the PVDF-casting solution. Antifouling properties of the composite membranes were evaluated via static protein adsorption test and UV-coupled ultrafiltration of BSA as model protein and extracellular polymeric substances (EPS) extracted from activated sludge of a pilot-scale membrane bioreactor (MBR), as the most significant biological factor responsible for membrane fouling. Performances of nanocomposite PVDF/TiO_2 and neat membranes were systematically compared so as to identify the benefic effect of TiO_2.

MATERIAL AND METHODS

Experimental Materials

Polymer polyvinylidene fluoride (PVDF pellet, molecular weight = 275,000 g.mol^{-1}) and solvent *N*,*N*–dimethylacetamide (DMAc, assay > 99.5%) were obtained from Sigma Aldrich. Pore-forming additive polyethylene glycol (PEG, molecular weight = 200 g.mol^{-1}) was supplied by Merck (Germany). TiO_2 Aeroxide® P25 nanoparticles (about 85% anatase-15% rutile, size of ca. 21 nm) and bovine serum albumin (BSA, molecular weight 67,000 g.mol^{-1}, assay > 98M) were also purchased from Sigma Aldrich. EPS was extracted from pilot-scale MBR-activated sludge of which was provided from a municipal wastewater treatment plant of Montpellier, France. Deionized (DI) water was obtained from Milli-Q system (Millipore Corp.) and used throughout the experiments.

BSA size[22] is up to 15 nm, while soluble EPS, extracted from MBR for these experiments, show two size distributions, one around 75 nm and the other around 750 nm (as shown in Figure 1). Size distribution curve of soluble EPS was obtained by Nanophox particle size analyzer (Sympatec, Germany).

Membrane Preparation

Nanocomposite membranes (T20) were prepared via nonsolvent-induced phase separation (NIPS) wet process. Casting solution was prepared by dissolving 5 wt. % PEG in 8.5 ml dimethylacetamide (DMAc) solvent, followed by the addition of 20 wt. % PVDF pellets. TiO_2 nanoparticle content corresponding to TiO_2/PVDF ratio of 20 wt. % was added to the above-mentioned casting solution. To avoid agglomeration and to obtain a well distribution of TiO_2 nanoparticles, casting solution was put in ultrasonic bath at 20°C for 20 min and then magnetically stirred for 24 h at 50°C and 100 rpm speed.

Casting solution was casted onto a glass plate covered with Teflon support (Approflon, France) using an automatic coater (K coater Erichsen, France) with a casting knife adjusted to 250 μm thickness and a casting speed of 4.66 cm/s and then immediately immersed into a distilled water bath at room temperature. After 3 hrs, prepared membranes were peeled off from the Teflon support and washed thoroughly with deionized water to remove residual solvent. Membranes were then kept in water before testing. Neat PVDF membranes, called T0, were prepared by the same protocol without TiO_2 nanoparticles.

Membrane Characterization

SEM and EDX Analysis. Morphology of prepared membranes was characterized by field emission scanning electron microscope (FESEM, Hitachi, S-4800, Japan). Membranes were cryogenically fractured in liquid nitrogen to obtain cross sections. Both surface and cross section of the membrane samples were sputter-coated with thin film of platinum to make them conductive. Existence of TiO_2 and its content on membrane surface was examined by energy-dispersive X-ray spectroscopy (FESEMw/EDS, Hitachi, S-4500, Japan).

Contact Angle Measurement. Contact angle (CA) measurements between water and the dry membrane were carried out with a contact angle meter (Automatic Contact Angle Meter, Model CA-VP, Kyowa Interface Science Co., Ltd., Japan) and a

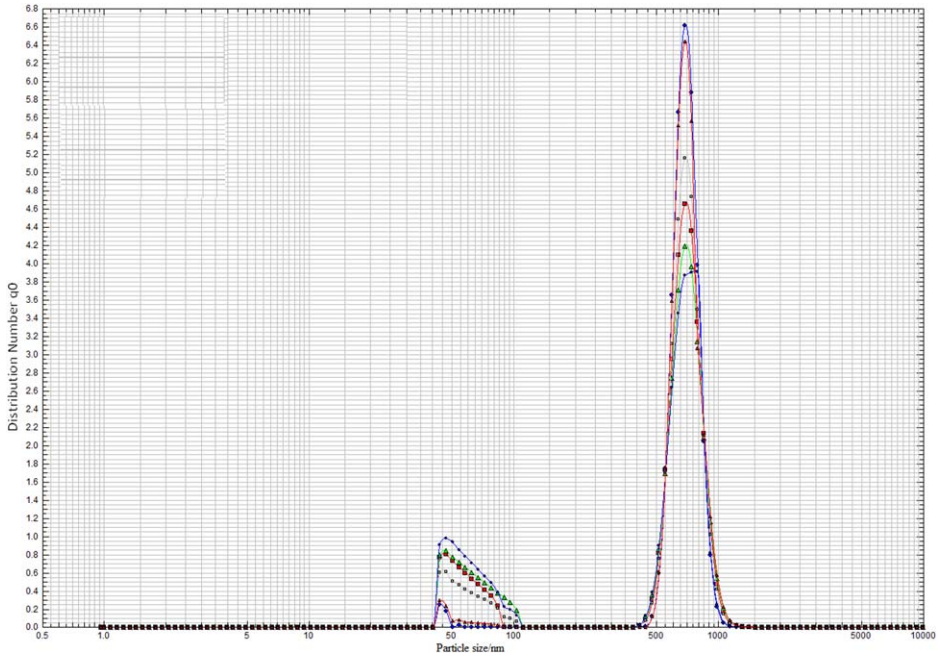

Figure 1. Particle size distribution of EPS solution extracted from laboratory scale MBR. [Color figure can be viewed in the online issue, which is available at wileyonlinelibrary.com.]

microscope image processing software (Image J, NIH-freeware version). Each sample was measured at least three times to obtain the average value.

Tensile Strength and Mechanical Properties. Mechanical properties of the membranes were determined using a tensile testing system (Zwick Roel, Germany), with a stretching rate of 10 mm/min at 20°C. Each sample was cut into 5 × 1 cm^2, and measurement was repeated for 5 times.

Permeability Test. Permeability tests were performed using dead-end stirred cell (Model 8400, Amicon Corp.) connected to an air-pressurized auxiliary 800-ml reservoir (Model RC800, Amicon Corp.). Effective membrane surface was 4.18 × $10^{-4}m^2$. Membranes were first conditioned in the test cell with Milli-Q water by gradually increasing the pressure up to 1.2 bar for 1.5 h. Permeate flux at 1 bar and 20°Cand permeability of membranes at 20°C were measured.

Static Protein Adsorption Experiments. Protein solution (1 g/L) was prepared by dissolving bovine serum albumin (BSA) in 0.1*M* phosphate buffer solution (PBS, pH 7.4). The membrane samples were cut into 7.5-cm-diameter round shape and soaked in PBS for 2 hrs. Then, they were suspended in glass Petri dishes containing 50 ml protein solution and were incubated in a thermostatic cabinet (AQUALYTIC, Germany) at 25°C for 24 h to reach equilibrium while agitating

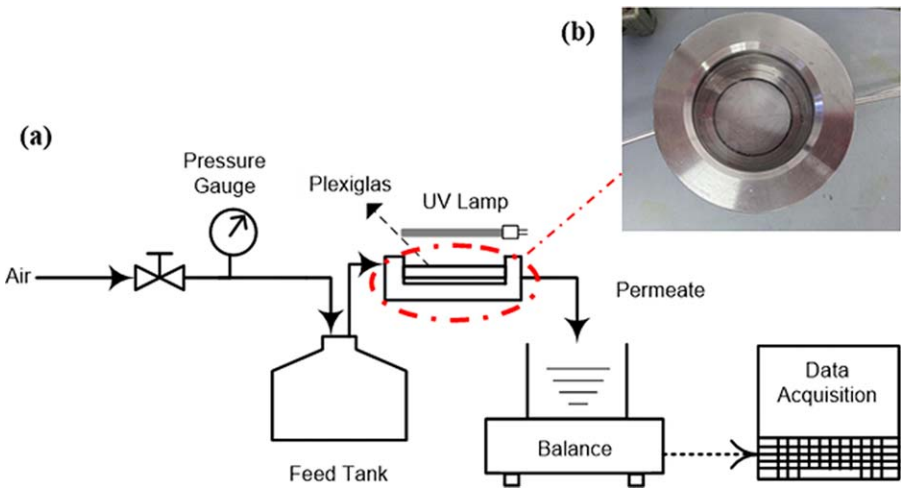

Figure 2. (a) Schematic description of the UV coupled dead-end UF system (b) Picture of the membrane cell with Plexiglas window suitable for direct UV irradiation during filtration. [Color figure can be viewed in the online issue, which is available at wileyonlinelibrary.com.]

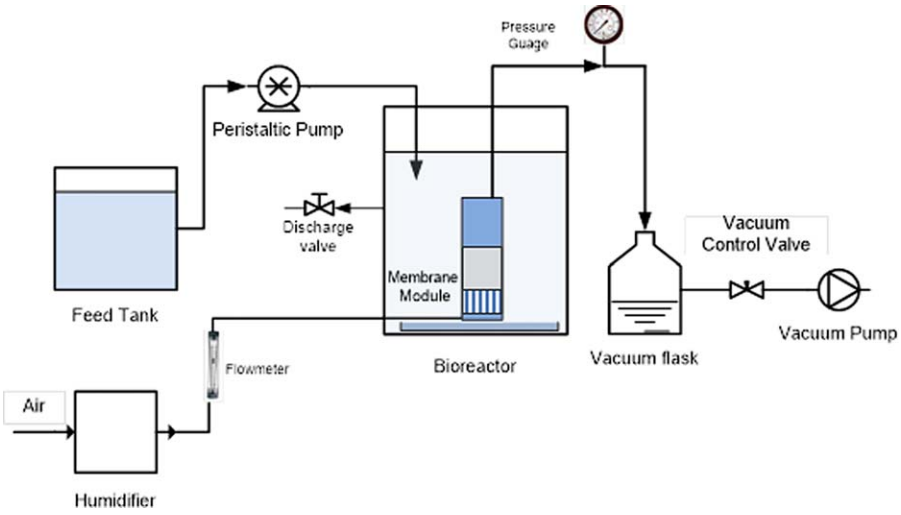

Figure 3. Submerged membrane bioreactor schematic diagram. [Color figure can be viewed in the online issue, which is available at wileyonlinelibrary.com.]

on a plate shaker at 240 rpm. The samples were frozen at −18°C on the day of collection and stored at this temperature prior to analysis. The modified Lowry method[23,24] was used to measure the concentrations of BSA in the solution before and after contacting with the membranes using a UV–Visible spectrophotometer (Shimadzu, UV2401PC). The calibration curve was used to determine the mass of protein (mg) on the membrane at 750 nm based on standard BSA solutions. A fresh standard curve ranging from 5–100 mg/L BSA was prepared with each measurement. The method quantification limit of adsorbed protein has been determined at 0.1 $\mu g/cm^2$.

The amount of protein adsorbed on the membrane was calculated by eq. (1). The data were averaged from two samples taken from the same membrane.

$$\text{Amount of protein adsorbed} = \frac{C_0 - C}{A} \times 100 \qquad (1)$$

where C_o and C μg/ml are the concentration of BSA solution before and after contacting with the membranes, respectively, and A (cm^2) is the membrane surface.

Following stabilized pure water fluxes were measured at 1 bar:

- before the adsorption test ($J_{w,0}$),
- immediately after 24 h of BSA adsorption test ($J_{w,ad}$),
- after 24 h of BSA adsorption test and a simple cleaning with water ($J_{w,ad,clean}$),
- after 24 h of BSA adsorption test, a simple cleaning with water and a UV irradiation of 30 min ($J_{w,ad,clean,UV}$).

Fouling Analysis of UV-coupled Ultrafiltration. UV coupled dead-end UF experiment was conducted in a laboratory scale filtration unit which is shown in Figure 2. A piece of Plexiglas was embedded on the top of the membrane cell which provided 11.9 cm^2 active surface for the membrane, and the membrane surface was irradiated by a 9W UV lamp (Philips, the Netherlands) during filtration experiment. The peak wavelength of UV lamp was 365 nm, and the intensity received by the membrane when it is inside the filtration cell filled with water is about 3.1 ± 0.3 mW/cm^2. Four sets of filtration experiment using two membranes (T0 and T20 with and without UV irradiation) for two different feed solutions, namely BSA solution and EPS solution extracted from activated sludge were performed. A new membrane sample was used for each filtration tests.

Bovine serum albumin solution (1 g/L) was prepared using 0.1*M* phosphate buffered at pH 7.4 as solvent. After permeability tests and determination of pure water flux $J_{w,0}$ (L m^{-2} h^{-1}), BSA solution was quickly replaced in the feed tank and the flux of BSA solution was measured. The flux for protein solution J_{BSA} (L m^{-2} h^{-1}) was measured at 1 bar for 1 h. Then, the fouled membranes were cleaned with distilled water for 20 min after the BSA

Table I. SMBR Feed Specification

Component	Purity (%)	Concentration (ppm)
C_6H_5OH	99	1000
K_2HPO_4	99	360
KH_2PO_4	99	280
NH_4Cl	99.9	200
$CaCl_2.6H_2O$	-	67
$MgSO_4.7H_2O$	98.5	248
$FeSO_4.7H_2O$	99.5	0.5

Table II. SMBR Operating Conditions

ParameterS	Amount
MLSS	5000-6000 mg/L
SRT	30-50 day
HRT	10-14 h
Permeate flux ($Lm^{-2}h^{-1}$)	10-15
Input phenol concentration	1000 mg/L
Input COD concentration	2300-2500 mg/L

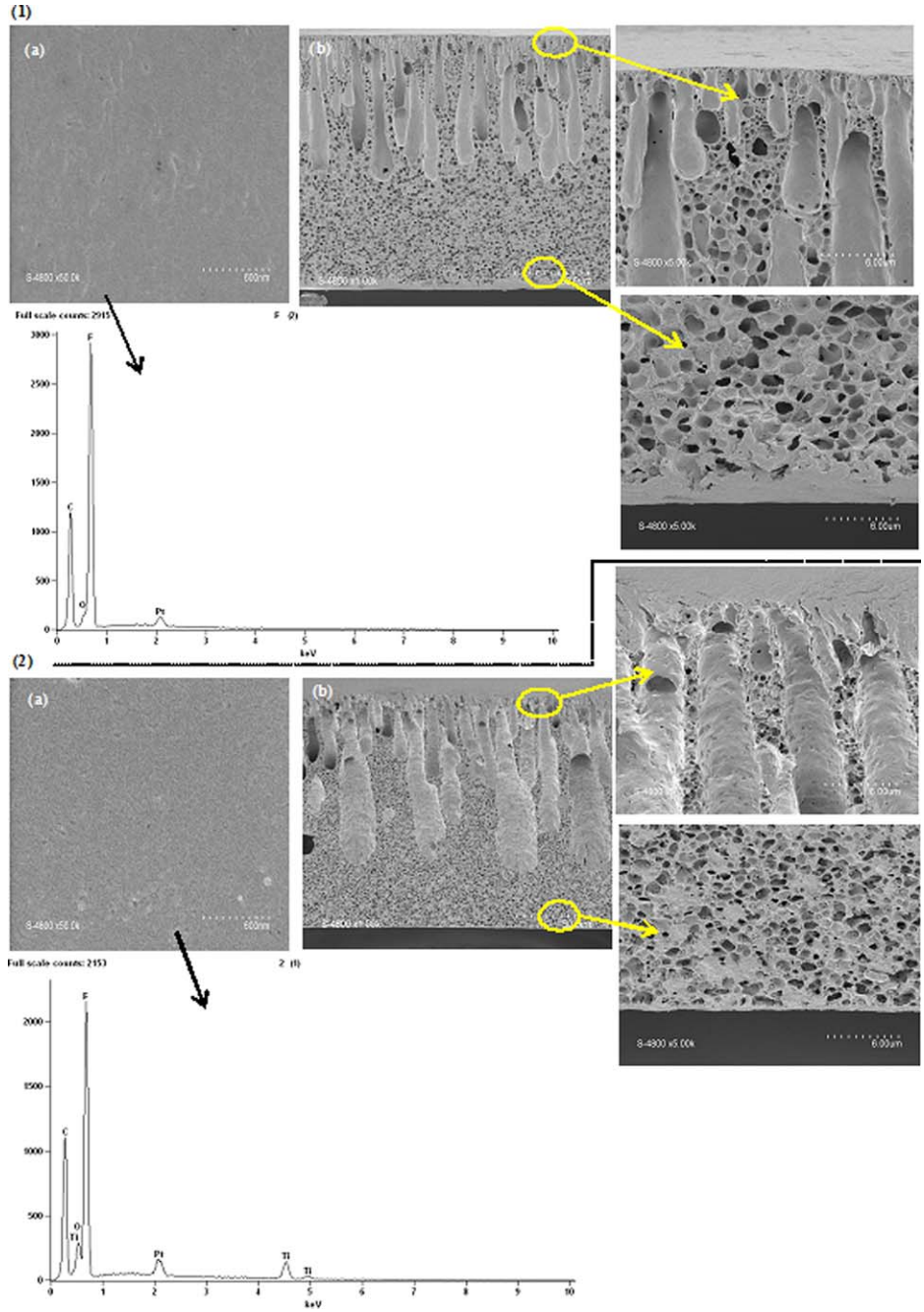

Figure 4. SEM images and EDX of composite PVDF membranes: (a) Top surface (b) cross-section of (1) PVDF–PEG membrane and (2) PVDF–PEG–TiO2 membrane. [Color figure can be viewed in the online issue, which is available at wileyonlinelibrary.com.]

filtration. The cleaning conducted by soaking the membrane in distilled water for 20 min, and then, it was washed twice with distilled water. Then, the water flux of the cleaned membranes $J_{w,\mathrm{BSA}}$ (L m^{-2} h^{-1}) was measured again. The BSA flux recovery ratio (FRR_{BSA}) will be estimated as follows:

$$\mathrm{FRR_{BSA}}(\%) = \left(\frac{J_{w,\mathrm{BSA}}}{J_{w,0}}\right)\times 100 \qquad (2)$$

Generally, higher FRR_{BSA} indicates better antifouling property of the membrane.

The BSA rejection ratio R_{BSA} is calculated by the following equation:

$$\mathrm{R_{BSA}}(\%) = \left(1-\frac{C_{p,\mathrm{BSA}}}{C_{f,\mathrm{BSA}}}\right)\times 100 \qquad (3)$$

where $C_{f,\mathrm{BSA}}$ and $C_{p,\mathrm{BSA}}$ represents protein concentrations in feed and permeate solution, respectively. The protein concentration is determined according to modified Lowry method using a UV-vis spectrophotometer.[23,24]

Extracellular polymeric substances (EPS), which are excreted by bacteria and composed of a variety of organic substances, are reported as a major controlling factor of membrane

Table III. Quantitative Results of EDX

Membrane	Weight percent concentration (%)			
	F	C	O	Ti
T0	53.7	43.8	2.5	0
T20	54.7	27.4	8.1	9.7

fouling in MBRs[11,25] In this study, soluble EPS were extracted from the mixed liquor in the MBR system of University of Montpellier 2 laboratory according to the thermal treatment method.[11] Before extraction, the mixed liquor of activated sludge was centrifuged at 4000 rpm for 5 min at 4°C in order to remove bulk solution and also concentrate the sludge. After discarding the supernatant, the remaining residue was resuspended in distilled water and centrifuged again at the same speed and conditions twice. The mixed liquor was then subject to the heat treatment (80°C, 0.5 h) and centrifuged again at 5000 rpm for 5 min at 4°C. The centrifuged supernatant is EPS solution, which can be used as feed solution in filtration test after dilution to 20 mg/L. The EPS solutions were stored at −18°C before use. To quantitatively analyze the membrane fouling performance, flux recovery ratio (FRR) and resistance of membranes was calculated as follows:

$$\mathrm{FRR_{EPS}}(\%) = \left(\frac{J_{w,\mathrm{EPS}}}{J_{w0}}\right)\times 100 \tag{4}$$

J_{w0} and $J_{w,\mathrm{EPS}}$ (L $m^{-2}h^{-1}$) are the pure water flux of membrane before fouling and after cleaning, respectively.

The EPS rejection ratio R_{EPS} is calculated by the following equation:

$$\mathrm{R_{EPS}}(\%) = \left(1-\frac{C_{f,\mathrm{EPS}}}{C_{p,\mathrm{EPS}}}\right)\times 100 \tag{5}$$

where $C_{p,\mathrm{EPS}}$ and $C_{f,\mathrm{EPS}}$ represents EPS concentrations in feed and permeate solution, respectively.

The EPS concentrations were measured by TOC Analyzer (Shimadzu, Japan).

Fouling behavior can be demonstrated by estimation of membrane resistance as shown below:[26]

- Membrane resistance: R_m (m^{-1})

$$\mathrm{R}_m = \frac{\mathrm{TMP}}{\mu\times J_{w0}} \tag{6}$$

where TMP is transmembrane pressure (in this case, 1 bar) and μ is permeate viscosity (Pa s).

- Irreversible resistance: R_{ir} (m^{-1})

$$\mathrm{R_{irBSA}} = \frac{\mathrm{TMP}}{\mu\times J_{w,\mathrm{BSA}}} - R_m \tag{7}$$

$$R_{\mathrm{irEPS}} = \frac{\mathrm{TMP}}{\mu\times J_{w,\ \mathrm{EPS}}} - R_m \tag{8}$$

- Reversible resistance: R_r (m^{-1})

$$R_{\mathrm{rBSA}} = \frac{\mathrm{TMP}}{\mu\times J_{\mathrm{BSA}}} - R_m - R_{\mathrm{irBSA}} \tag{9}$$

$$R_{\mathrm{rEPS}} = \frac{\mathrm{TMP}}{\mu\times J_{\mathrm{EPS}}} - R_m - R_{\mathrm{irEPS}} \tag{10}$$

Where J_{BSA} and J_{EPS} (L m^{-2} h^{-1}) are the BSA and EPS filtration flux, respectively.

- Total resistance: R_t (m^{-1})

$$R_t = R_m + R_{ir} + R_r \tag{11}$$

MBR Experiments. The effect of TiO_2 on the performance of the PVDF membrane has been studied in a submerged membrane bioreactor (SMBR) as shown in Figure 3. The TMP increase was investigated at constant flux for effective membrane area of 50 cm^2. The SMBR feed specification and operating conditions were illustrated in Tables I and II, respectively.

Chemical cleaning of the membrane was performed when the transmembrane pressure (TMP) reached 0.4 bar, according to the protocol reported by Nguyen *et al.* using 10m*M* SDS solution for 45 min.[27] In this way, the fouled membranes were backwashed by placing them upside down in the filtration cell and applying 0.1 bar vacuum for 5 min. The backwashed membranes were then soaked with gentle shaking in solutions of 10m*M* SDS solution at 24°C for 45 min. The pure water flux of the chemically cleaned membranes was determined after rinsing them thoroughly with distilled water.

RESULTS AND DISCUSSION

Membrane Characterization

Membrane Morphology. T20 nanocomposite PVDF/TiO_2 membrane and T0 neat PVDF membrane were first morphologically characterized. Effect of the addition of TiO_2 nanoparticles on the membrane structure was observed by SEM. Cross sectional and top surface of prepared membranes are shown in Figure 4. Cross-sectional images in Figure 4 show that both prepared membranes present a typical asymmetric structure consisting of a thin, dense top layer and a porous sublayer divided into finger-like macrovoids and a sponge-like structure as reported in previous researches.[8]

Finger-like macrovoids for nanocomposite membrane T20 were larger and longer with uniform shape from top to bottom while they were smaller for the neat membrane T0.

Table IV. Tensile Strength and Elongation at Break of T0 and T20 Membrane

Membrane	Tensile strength (MPa) ± SD	Elongation at break (%) ± SD
T0	2.49 ± 0.35	46.58 ± 5.82
T20	3.13 ± 0.12	92.44 ± 3.93

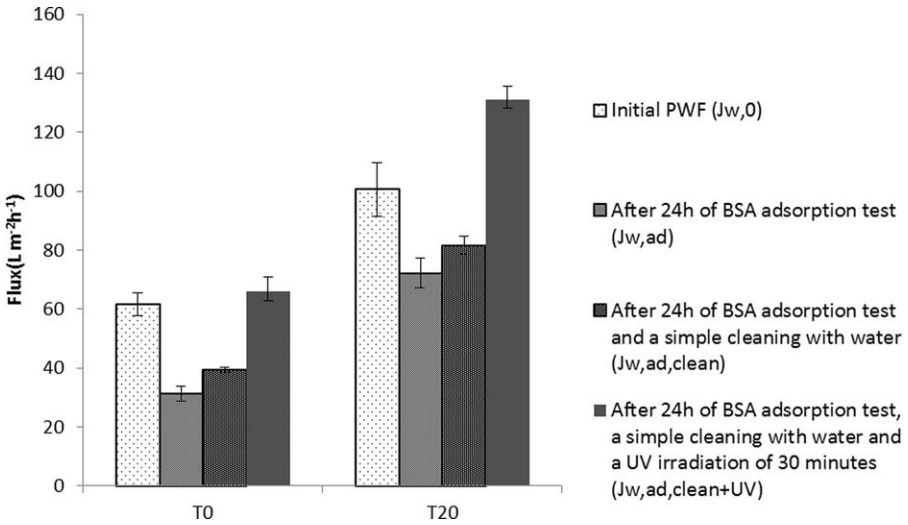

Figure 5. Change in stabilized flux of the BSA adsorbed neat (T0) and nanocomposite (T20) membranes before and after BSA static adsorption. Bars represent standard deviations.

In the sponge-like section of the nanocomposite membrane, pores seem smaller in size but existed in large quantities which could result in more porosity, whereas they were larger for the neat membrane as shown in the magnified images of Figure 4.

By adding TiO_2 to the dope solution, hydrophilic properties of the nanoparticles induce higher water penetration and solvent departure, during the phase separation process that favors formation of larger finger-like macrovoids instead of the sponge-like structure. Furthermore, interfacial stress between polymer and nanoparticles causes the formation of pores as consequences of shrinkage of polymer phase during demixing process resulting in a more porous sponge-like structure. Furthermore, the dense, skin layer thickness seems to decrease with the addition of TiO_2 as observed by Bian *et al.*[28]

Evidence of TiO_2 in the Nanocomposite Membrane. The presence of TiO_2 in the membrane was investigated by energy dispersion of X-ray analysis (EDX Point) which confirms the existence of TiO_2 both on the top surface and cross section of the composite membrane. A peak observed around 4.5 keV belongs to Ti and the peak around 0.7 keV belongs to Fluor which comes from PVDF. Ti peaks can be observed in the spectrum of the nanocomposite membrane as shown in Figure 4. EDX of the neat PVDF membrane is illustrated for comparison.

Quantitative results of EDX are presented in Table III. Moreover, Ti theoretical amount was estimated using the following equation:

$$m_{\mathrm{Ti}} = \frac{M_{\mathrm{Ti}}}{M_{\mathrm{TiO_2}}} \times x_{\mathrm{TiO_2}} \times m_{\mathrm{PVDF}} \tag{12}$$

where m_{Ti} is the mass of Ti, M_{Ti} is the molar mass of Ti, $M_{\mathrm{TiO_2}}$ is the molar mass of TiO_2, $x_{\mathrm{TiO_2}}$ is the weight percentage of TiO_2 (20% in this case), and m_{PVDF} is the mass of PVDF (2 g in this case). Ti weight percentage in the membrane is then calculated using eq. (13):

$$\%\mathrm{wt\ Ti} = \frac{m_{\mathrm{Ti}}}{m_{\mathrm{TiO_2}} + m_{\mathrm{PVDF}}} \tag{13}$$

Where $m_{\mathrm{TiO_2}}$. is the mass of TiO_2 in the membrane.

Theoretical and experimental values were found to be very close: 9.98 and 9.7%, respectively. This could indicate that TiO_2 loss is limited during the elaboration process.

Membrane Hydrophilicity. Contact angle of the neat PVDF membrane ($81.2 \pm 0.3°$) decreases with the addition of TiO_2 ($60.7 \pm 0.4°$) implying that hydrophilicity and/or smoothness of the membrane was improved by the incorporation of TiO_2 nanoparticles. The contact angle of the composite membrane decreased due to the presence of –OH functional groups of TiO_2.[29]

Mechanical Property. Mechanical property of neat PVDF membrane (T0) and PVDF/TiO_2 (T20) nanocomposite membrane has been studied in terms of tensile strength and tensile elongation at break as shown in Table IV.

As shown in the table, the presence of TiO_2 nanoparticles enhanced the mechanical strength. As reported by Ong *et al.*,[30] TiO_2 is a suitable additive for the improvement of mechanical property of PVDF membranes due to its excellent mechanical properties, high surface area, and high aspect ratio. Indeed, the higher viscosity of the casting suspension is another reason for the more mechanical strength of the composite membranes. Similar observations were reported by Yang *et al*[31], and Zhou *et al.*[32] in the case of TiO_2 polysulfone and PVDF composite membranes, respectively.

Permeability Test. Permeability of TiO_2 nanocomposite membrane was about two times higher than that of the neat PVDF membrane, 100.0 ± 3.5 $L.h^{-1}.m^{-2}.bar^{-1}$ for the composite membrane versus 50 ± 1.5 $L.h^{-1}.m^{-2}.bar^{-1}$ for the neat membrane. As discussed in previous sections, the presence of TiO_2 in the membrane matrix results in more porous membranes with larger finger-like macrovoids comparing to PVDF neat

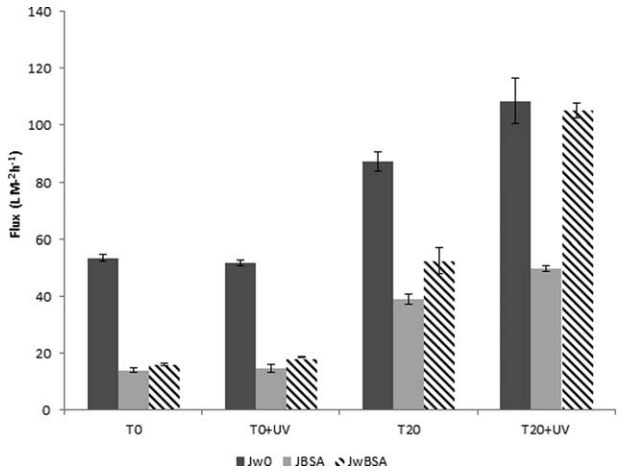

Figure 6. Water and protein (BSA) filtration flux for neat (T0) and nanocomposite (T20) membrane with and without UV irradiation. Bars represent standard deviations.

membrane, which enhanced membrane permeability. In addition, hydrophilicity and smoothness improvement due to TiO_2 nanoparticules promote passage of pure water flux and thus participates to the improvement of membrane permeability.

Fouling Analysis. ***Static protein adsorption.*** Membrane behavior toward soluble foulant compounds has been investigated using commercial BSA and static adsorption tests.[33]

After 24 h of contact between 1 g/L BSA solution and the manufactured membrane, adsorbed amount of protein on the neat PVDF membrane was about 539 $\mu g/cm^2$ and 349 $\mu g/cm^2$ on the nanocomposite membrane. Thus, TiO_2/PVDF membranes have been found to have 35.3% lower protein adsorption, which can be related to the increase in the membrane surface hydrophilicity and the decrease in membrane roughness as previously found with contact angle measurement.[9] Lower affinity between membrane surface and protein could explain this behavior. The membrane permeability before and after static BSA adsorption were measured. The results are shown in Figure 5.

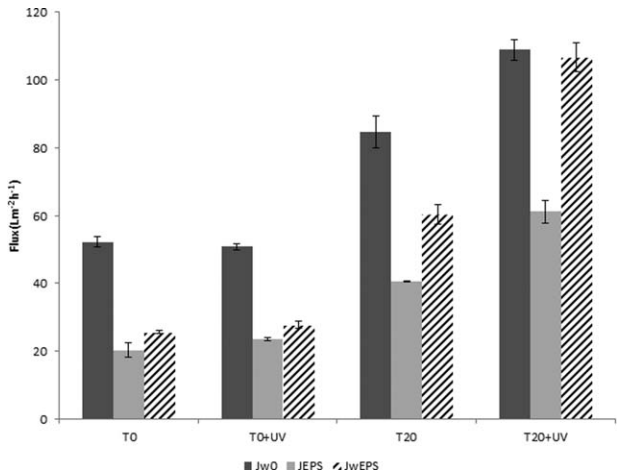

Figure 7. Water and Extra Polymeric Substances (EPS) filtration flux for neat (T0) and nanocomposite (T20) membrane with and without UV irradiation. Bars represent standard deviations.

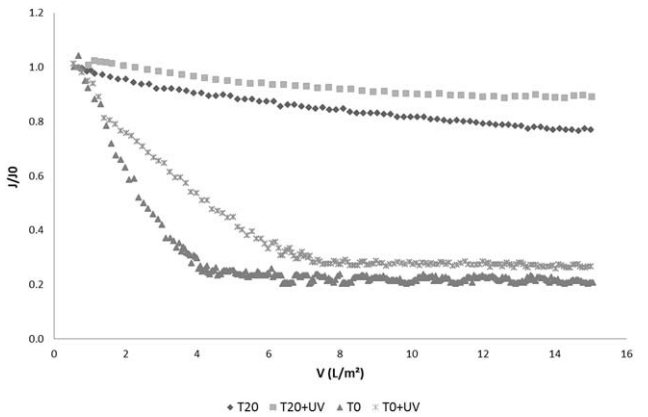

Figure 8. Normalized flux decline trend of neat (T0) and TiO2/PVDF nanocomposite membranes during protein (BSA) ultra-filtration with and without simultaneous UV irradiation.

The pure water flux declines after BSA adsorption for both membrane but is more important for the neat PVDF membrane; it confirms that more protein adsorption occurs on PVDF membrane surface compared with nanocomposite membrane. Simple water cleaning does not significantly improve membrane flux recovery. A 30 min UV irradiation led to a full recovery of the flux through nanocomposite membrane. UV irradiation was performed after simple water cleaning, and the membranes were soaked in a Petri dish filled with distilled water and the surface of the membrane was UV irradiated for 30 min. The UV lamp was located on the edge of the Petri dish, and the whole Petri dish and the lamp were covered by a box.

UV static irradiation has a benefic effect in both case but much more pronounced for nanocomposite membrane. This result was also observed by Damodar *et al.*[16] It can be supposed that UV irradiation could alternate BSA protein[34] and thus adsorption affinity that enables the recovery of major part of the initial flux of membrane. In addition, activation of photocatalytic and superhydrophilic TiO_2 properties under UV enable a gain in the filtration performance.

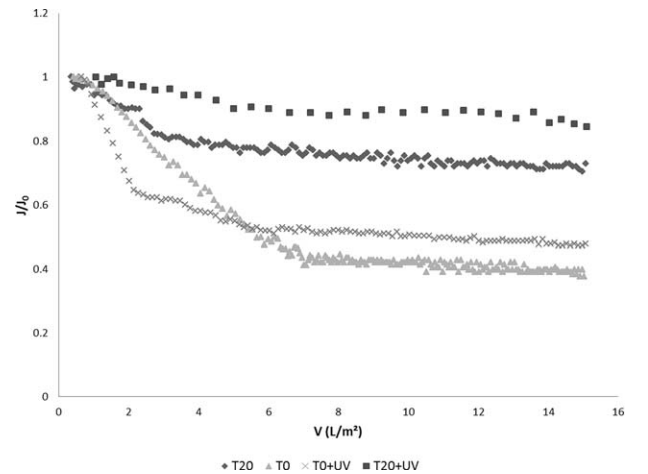

Figure 9. Normalized flux decline trend of neat (T0) and TiO2/PVDF nanocomposite membranes during EPS ultra-filtration with and without simultaneous UV irradiation.

Table V. Change in Fouling Resistances, Flux Recovery Ratio and Rejection During BSA Filtration Coupled with Simultaneous UV Irradiation

Membranes	Rejection (%)	FRR %	R_m($\times 10^{12}$ m^{-1})	R_{rev}($\times 10^{12} m^{-1}$)	R_{irrev}($\times 10^{12}$ m^{-1})	R_t ($\times 10^{12}$ m^{-1})
T0	67.3	32.0	8.67	1.19	15.98	25.84
T0 + UV	62.8	35.7	6.98	5.13	12.57	24.68
T20	88.2	60.2	4.13	2.40	2.73	9.26
T20 + UV	85.6	96.9	3.32	3.81	0.11	7.24

The pure water flux (PWF) of nanocomposite membrane after UV irradiation was higher than the initial PWF. This phenomenon can be explained based on the probable superhydrophilicity induced by TiO_2 nanoparticles entrapped in the PVDF membrane matrix as reported by Takeuchi *et al.*[35]

Fouling analysis of UV-coupled ultrafiltration. For these experiments, same synthetic solution with commercial BSA was used. In addition, real EPS solution was prepared as soluble EPS have been found to be major responsible for fouling.[9,36] To further investigate the membranes fouling resistance, BSA and EPS filtration was performed with and without UV irradiation. Figures 6 and 7 present stabilized flux J_{BSA} and J_{EPS}, respectively. Jw_0 is the pure water flux after stabilization.

As shown in Figures 6 and 7, Jw_0 corresponding to nanocomposite membrane was higher comparing to the neat PVDF membrane due to hydrophilicity and porous structure improvement with TiO_2. Jw_0 is much more improved under UV irradiation for composite membrane because of activation of superhydrophilicity properties as explained elsewhere.[37,38] Consequently, J_{EPS} decline is less pronounced under UV than in darkness conditions for nanocomposite membrane: 51% against 44% for EPS. However, it is not significant for J_{BSA}. This is confirmed by Figures 8 and 9 which present normalized BSA and EPS filtrate flux ratio (J/J_0) during the constant pressure (1 bar) filtration of BSA and EPS solution versus filtrate volume.

For T0 membrane, there is a sharp decrease in the permeate flux until stabilized flux is reached around 4–6 (Lm^{-2}). Flux stabilization is reached much more rapidly for nanocomposite membrane T20. Moreover, stabilized flux is higher for nanocomposite membrane (Figures 8 and 9).

From these figures, it can be concluded that the nanocomposite membrane presented better BSA and EPS filtration performance under UV irradiation and the neat PVDF membrane exhibited worse flux decline. The flux after 1 h of filtration of BSA and EPS declined by 79.2% and 62.2%, respectively, on the neat membrane, while these values are 23% and 27.1% on the nanocomposite membrane without UV irradiation. The flux decline observed during the BSA filtration is due to the combined effects of BSA adsorption on or within the membrane pores, BSA deposition during filtration and BSA concentration polarization.[39] An increase in the membrane hydrophilicity as a result of TiO_2 entrapment and UV irradiation were beneficial for preventing the fouling caused by both BSA and EPS.

After water cleaning, the fluxes $J_{w,BSA}$ and $J_{w,EPS}$ were obtained. Flux recovery ratio (FRR) was calculated to assess the fouling resistance of the membranes for both BSA and EPS filtration. The results are shown in Table V and VI for BSA and EPS filtration, respectively. According to the obtained results, the flux recovery ratio after water cleaning, following both BSA and EPS filtration is much higher for nanocomposite membrane than for the PVDF membrane. For example, FRR_{BSA} is about 32% for the T0 membrane, while it reaches 60% for the T20 membrane. The higher FRR values confirm the better antifouling property of the prepared nanocomposite membranes.

FRR_{EPS} and FRR_{BSA} for the neat PVDF membrane were not significantly improved by the UV irradiation. On the contrary, the combined water/UV cleaning of composite membrane is much more efficient (up to 97%–98%) than the sole water cleaning (60%–71%).

It can be related both to the photodegradation of organic matter (BSA, EPS) by the TiO_2/UV association and to the improvement of water penetration through the membrane under UV irradiation which improves membrane cleaning.

BSA and EPS rejection rate is higher for TiO_2/PVDF membrane than for PVDF membrane as shown in Tables V and VI. Concerning nanocomposite membrane, BSA rejection rate was 88.2% compared to 67.3% for the neat PVDF membranes. Nonetheless, as observed by Bian *et al.*,[28] it seems that pore size is not significantly modified by TiO_2 addition. However, membrane surface properties modification (hydrophilic and/or smoothness) could explain the better rejection rate of BSA and

Table VI. Change in Fouling Resistances, Flux Recovery Ratio and Rejection During EPS Filtration Coupled with Simultaneous UV Irradiation

Membranes	Rejection (%)	FRR %	R_m($\times 10^{12}$ m^{-1})	R_{rev}($\times 10^{12}$ m^{-1})	R_{irrev} ($\times 10^{12}$ m^{-1})	R_t($\times 10^{12}$ m^{-1})
T0	63.6	49.1	6.89	3.75	7.14	17.78
T0 + UV	64.7	54.7	7.09	2.36	5.86	15.31
T20	84.4	71.2	4.25	2.88	1.72	8.85
T20 + UV	82.0	98.1	3.31	2.52	0.07	5.89

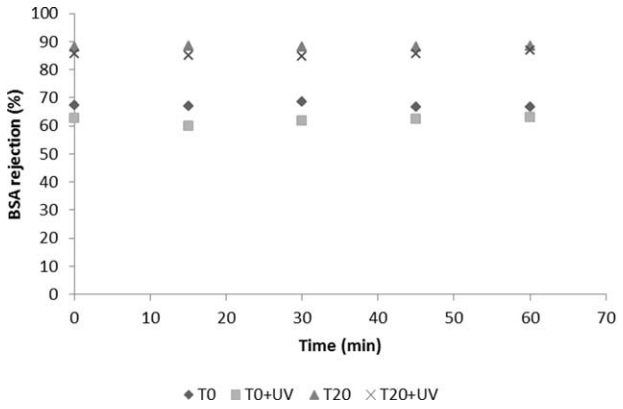

Figure 10. BSA removal on T0 and T20 membranes during UV coupled ultrafiltration.

EPS for T20 membrane (see section Membrane Hydrophilicity). Indeed, using more hydrophilic membrane leads to higher permeate flux and thus higher rejection rates (passage of water molecules is favored compared to organic matter molecules). However, a possible photocatalytic degradation of foulant (BSA and EPS) may also results in higher retention and was reported by Nguyen *et al.*[40] and Zhang *et al.*,[41] too. They showed that immobilized titanium dioxide in the matrix of membranes under UV irradiation improves the antifouling property of the membranes through photocatalytic degradation of the foulants prior to reaching the membrane surface.

On the other hand, Teow *et al.*[42] showed that variation in membrane properties such as surface charge, using TiO_2 nanoparticles, affects the physic–chemical interactions of membrane and its feed solution. They showed that the presence of TiO_2 nanopaticles increases net negative charge on the surface of PVDF/TiO_2 composite membranes. Based on Lin *et al.*[36]review article and Salgin *et al.*,[43] EPSs and BSA has negative charge at near neutral pH. Hence, the electrostatic repulsion between such folulants and TiO_2 particles on the surface of the membranes results in higher EPS and BSA retention. Therefore, it can be concluded that higher retention caused by the surface charge and hydrophilicity modification and a possible photocatalytic degradation of foulant (BSA and EPS).

Resistances analysis (Table V) confirms that the reduction in total resistance (R_t) of the composite TiO_2/PVDF membrane is effective under UV irradiation. Fouling resistance is due to reversible (R_r) and irreversible (R_{irr}) protein adsorption.

Table VI shows that the irreversible resistance of composite membrane can be successfully decreased by around 0.11×10^{12} m^{-1} through coupled UV irradiation/filtration of BSA. In the case of EPS filtration, the irreversible fouling resistance ($0.07 \times 10^{12}\ m^{-1}$) was lower than the corresponding value for BSA filtration and nanocomposite membrane under UV irradiation showed relatively high fouling reduction up to about 99% compared to neat PVDF membrane.

In order to investigate the effect of UV irradiation on TiO_2/PVDF membrane surface during the UV coupled ultrafiltration experiments, the removal rates of BSA and EPS on the neat T0 and T20 nanocomposite membranes under UV irradiation during 1 h of filtration time were measured and the results were shown in Figures 10 and 11. The results showed that the removal rates have no obvious change during entire 1 h UV irradiation. Similar results were reported by Song *et al.*,[9] to confirm stability of the PVDF/TiO_2 membranes during a limited period of time under UV irradiation. However, the effect of long-term UV irradiation on the membranes surface has not been investigated yet, and it is the subject of our future work.

As mentioned, the application of UV irradiation to investigate fouling reduction effect of TiO_2 nanocomposite polymeric membranes have been the subject of some research activities as summarized in Table VII. Performance of the membranes for different proteins and EPS extracted from MBR activated sludge have been also studied as shown in Table VII. The positive effect of UV irradiation on the performance of TiO_2 entrapped membranes can obviously be observed. For example, Damodar *et al.*[16] reported a FRR of 98% for BSA filtration by 30 min UV irradiation using a PVDF/TiO_2 membrane. The EPS filtration experiments without UV irradiation for a PSF membrane were performed by Guoliang Zhang *et al.*[11] and the results showed about 18% improvement in FRR by addition of 3 wt. % TiO_2 to the PSF membrane matrix. Guojun Zhang *et al.* also studied the static EPS adsorption (extracted from activated sludge) under six operational conditions using a neat PVDF membrane without UV irradiation and compared the FRRs.[44] None of the above-mentioned researchers studied the effect of UV irradiation on the TiO_2/PVDF membranes in a continuous manner during filtration of real EPS extracted from MBR pilot application as performed in this study. As can be observed in Table VII, the FRR values in similar studies hardly reach 90%, while by applying the materials and the methods used in this study, the FRR of the membrane can be improved about 20%.

MBR fouling. The result of TMP increase due to membrane fouling in a submerged membrane reactor was illustrated in Figure 12. As shown in the figure, the presence of TiO_2 nanoparticles reduced the fouling potential of the membrane significantly and improved the performance of PVDF membrane in

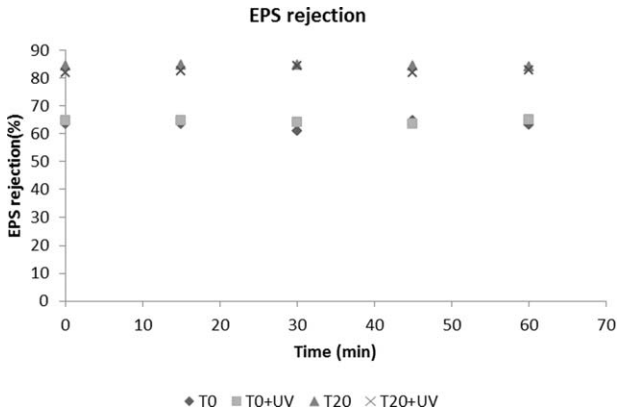

Figure 11. EPS removal on T0 and T20 membranes during UV coupled ultrafiltration.

Table VII. Fouling Analysis of TiO_2-Entrapped Polymeric Membranes Studied in Previous Researches as Compared to This Study

Membrane material	Polymer (wt. %)	Solvent/ pore former	TiO_2 (wt. %)	Foulant	FRR (%)						Ref.
					UV Irradiation			Without UV irradiation			
PVDF(Solef 6020,Solvay)	12	DMAc/PEG 600	0.5	NOM[a]	1 h	2 h	4 h	54			[9]
					69	71	90				
PVDF	10	NMP	1	BSA	94			83			[16]
			2		98.7			97.5			
			4		98			96.3			
PVDF(Solef)	18	DMAc	1.5	MB[b]	0.5 h	1 h		91.3			[21]
					95	100					
PSF(Shugung Chemical Factory, China, Mw=65,000 g/mol)	17	DMAc/PEG2000	3	BSA	-			77			[11]
				EPS				80			
PES (Ultrason E6020P, Mw=58,000 g/mol)	16	DMAc/PVP	2	Nonskim milk	74			66			[37]
			4		75			64			
			6		69			63			
PVDF[c]	-	-	0	EPS extracted from activated sludge[d]				After 1 h ads.	After 2 h ads.	After 3 h ads.	After 4 h ads.	After 5 h ads.	[44]
				A				88.34	82.36	75.88	72.71	72.56	
				B				84.99	74.52	67.78	64.27	63.64	
				C				85.06	68.38	66.61	63.25	63.02	
				D				78.14	68.00	55.05	54.10	53.16	
				E				77.67	65.84	56.96	49.46	48.79	
				F				76.84	61.32	51.30	45.24	43.64	
PVDF (Sigma Aldrich, Mw=275,000 g/mol)	20	DMAc/PEG200	20[e]	BSA	96.9			60.2					This study
				EPS	98.1			71.2					

[a] Methylene blue.
[b] Natural organic matter.
[c] (100,000 MWCO membrane provided by Research Center for Eco-Environmental Science, Chinese Academy of Science).
[d] EPS of the sludge samples were extracted under six different conditions for more information see Table I of reference 36.
[e] TiO_2/PVDF.

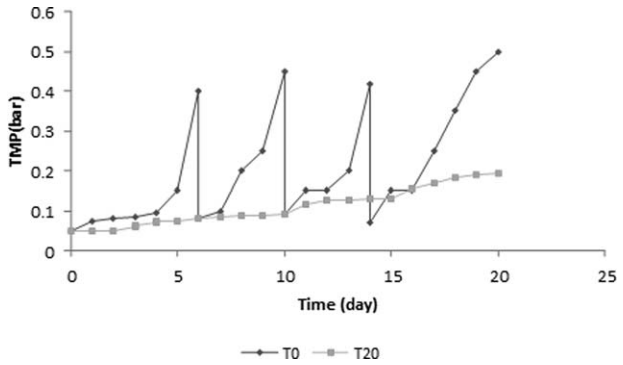

Figure 12. TMP increase for T0 and T20 membranes in MBR.

SMBR system. During the period of study (20 days), the neat PVDF (T0) membrane cleaned three times following TMP increase due to membrane fouling, while the slope of TMP increase for nanocomposite membrane (T20) was so slight that it did not need cleaning. This observation is in consistence with the results of BSA and EPS filtration (previous section) which confirmed that lower cleaning frequency is required for TiO_2/PVDF nanocomposite membrane comparing the neat PVDF membrane.

CONCLUSION

PVDF-TiO_2 nanocomposite membranes with PEG as additive was prepared via phase inversion by dispersing TiO_2 nanoparticles into the PVDF matrix. Different techniques such as SEM, EDX, and contact angle measurement were applied to characterize the membranes. Moreover, flux performances and antifouling properties of the nanocomposite membrane toward BSA, as a model protein, and EPS, as the most important biological factor responsible for MBR fouling, were evaluated in dead-end filtration experiments with and without UV irradiation through a Plexiglas window.

Prepared composite membranes have a typical asymmetric structure with larger and longer macrovoids than for neat PVDF membrane resulting in increased pure water permeability also due to hydrophilicity and smoothness improvement from TiO_2 presence.

Static protein adsorption experiment confirms that nanocomposite membranes had remarkably reduced protein adsorption capacity, probably because of a higher surface hydrophilicity. UV static irradiation enables the full recovery of initial flux of composite membranes which thus present self-cleaning ability.

The effect of continuous UV irradiation during filtration of pure water, BSA, and EPS solutions was investigated. It appears that dynamic UV irradiation has an effect only on nanocomposite membranes for which initial flux is increased.

In comparison with neat PVDF membranes, composite membranes reach flux stabilization very rapidly both in darkness and UV conditions. Moreover, hydrophilic properties of these membranes and photocatalytic degradation lead to better retention performances of BSA and EPS which are still improved under UV irradiation. Composite membranes under UV irradiation presented the best flux recovery ratio confirming the antifouling property of such membranes when filtration is combined with UV irradiation at 365nm. Finally, the results of MBR-fouling experiments showed that lower cleaning frequency is required for TiO_2/PVDF nanocomposite membrane comparing the neat PVDF membrane. Hence, it can be concluded that Immobilization of TiO_2 nanoparticles in organic membranes is thus a simple and powerful method for fouling mitigation in MBR application.

AUTHOR CONTRIBUTIONS

Mrs. Maryam Tavakolmoghadam prepared the membranes and conducted the characterization and fouling analysis experiments and wrote the draft of manuscript; Dr. Geoffroy Lesage and Prof. Toraj Mohammadi supervised the research and reviewed and edited the manuscript critically; Dr. Jean-Pierre Mericq and Dr. Julie Mendret advised in membrane preparation and provided the UV-coupled dead-end set-up and revised the manuscript. Dr. Marc Heran supported the experiments relating to EPS extraction and MBR pilot maintenance. Prof. Catherine Faur and Prof. Stephan Brosillon advised in the field of UV irradiation and performed the UV-Lamp intensity measurements. Dr. Mahmud Hemmati and Dr. Freshteh Naeimpoor advised and supported the research scientifically in polymeric aspects and biological fields, respectively.

REFERENCES

1. Nath, K. In Membrane Separation Processes. Prentice Hall of India Private Limited: New Delhi, **2008**; Chapter *5*, pp 117.
2. Drews, A. *J. Membr. Sci.* **2010**, *363*, 1.
3. Rana, D.; Matsuura, T. *Chem. Rev.* **2010**, *110*, 2448.
4. Liu, C.; Caothien, S.; Hayes, J.; Caothuy, T.; Otoyo, T.; Ogawa, T. In Membrane Chemical Cleaning: From Art to Science. Pall Corporation: **2006**; pp 1.
5. Le-Clech, P.; Chen, V.; Fane, T. A. G. *J. Membr. Sci.* **2006**, *284*, 17.
6. Meng, F.; Chae, S.; Drews, A.; Kraume, M.; Shin, H.; Yang, F. *Water Res.* **2009**, *43*, 1489.
7. Kim, J.; Van der Bruggen, B. *Environ. Pollut.* **2010**, *158*, 2335.
8. Liu, F.; Hashim, N. A.; Liu, Y.; Moghareh Abed, M. R.; Li, K. *J. Membr. Sci.* **2011**, *375*, 1.
9. Song, H.; Shao, J.; Hea, Y.; Liu, B.; Zhong, X. *J. Membr. Sci.* **2012**, *405*, 48.
10. Teow, Y. H.; Ahmad, A. L.; Lim, J. K.; Ooi, B. S. *J. Appl. Poly. Sci.* **2013**, *128*, 3184.
11. Zhang, G.; Lu, S.; Zhang, L.; Meng, Q.; Shen, C.; Zhang, J. *J. Membr. Sci.* **2013**, *436*, 163.
12. Razmjou, A. The Effect of TiO2 Nanoparticles on the Surface Chemistry, Structure and Fouling Performance of Polymeric Membranes, Ph. D. Thesis, School of Chemical

Engineering, The University of New South Wales, Sydney, Australia, **2012**.

13. Chong, M. N.; Laera, G.; Jin, B. Integrating Membrane Bioreactor with Advanced TiO2 Photocatalytic Technology for the Removal of Pharmaceutical Drugs from Recycled Wastewater. in 9th IWA Leading Edge Conference on Water and Wastewater Technologies. Australia, **2012**.
14. Laera, G.; Chong, M. N.; Jin, B.; Lopez, A. *Bioresource Technol.* **2011**, *102*, 7012.
15. Mozia, S. *Sep. Purif. Technol.* **2010**, *73*, 71.
16. Damodar, R. A.; You, S. J.; Chou, H. H. *J. Hazard. Mater.* **2009**, *172*, 1321.
17. Bae, T.; Tak, T. M. *J. Membr. Sci.* **2005**, *249*, 1.
18. Cao, X.; Ma, J.; Shi, X.; Ren, Z. *Appl. Surf. Sci.* **2006**, *253*, 2003.
19. Oh, S. J.; Kim, N.; Lee, Y. T. *J. Membr. Sci.* **2009**, 345, *13*.
20. Rahimpour, A.; Jahanshahi, M.; Rajaeian, B.; Rahimnejad, M. *Desalination* **2011**, *278*, 343.
21. Ngang, H. P.; Ooi, B. S.; Ahmad, A. L.; Lai, S. O. *Chem. Eng. J.* **2012**, *197*, 359.
22. Wright, A. K.; Thompson, M. R. *Biophys. J.* **1975**, *15*, 137.
23. Frølund, B.; Griebe, T.; Nielsen, P. H. *Appl. Microbiol. Biotechnol.* **1995**, *43*, 755.
24. Lowry, O. H.; Rosebrough, N. J.; Fan, A. L.; Randall, R. J. *J. Biol. Chem.* **1951**, *193*, 65.
25. Menniti, A.; Kang, S.; Elimelech, M.; Morgenroth, E. *Water Res.* **2009**, *43*, 4305.
26. Razmjou, A.; Mansouri, J.; Chen, V. *J. Membr. Sci.* **2011**, *378*, 73.
27. Nguyen, S. T.; Roddick, F. A. *Desalin. Water Treat.* **2011**, *34*, 94.
28. Bian, X.; Shi, L.; Yang, X.; Lu, X. *Ind. Eng. Chem. Res.* **2011**, *50*, 12113.
29. Yune, P. S.; Kilduf, J. E.; Belfort, G. *J. Membr. Sci.* **2011**, *377*, 159.
30. Ong, C. S.; Laua, W. J.; Goh, P. S.; Ng, B. C.; Ismail, A. F. *Desalin. Water Treat.* **2013**, *1*.
31. Yang, Y.; Zhang, H.; Wang, P.; Zheng, Q.; Li, J. *J. Membr. Sci.* **2007**, *288*, 231.
32. Zhou, Q.; Li, J.; Yan, B.; Wu, D.; Zhang, Q. *Chin. J. Polym. Sci.* **2014**, *32*, 892.
33. Iritani, E.; Tachi, S.; Murase, T. *Colloid Surf. A* **1994**, *89*, 15.
34. Porter, D. D.; Maurer, P. H. *Photochem. Photobiol.* **1962**, *1*, 91.
35. Takeuchi, M.; Sakamato, K.; Martra, G.; Coluccia, S.; Anpo, M. *J. Phys. Chem. B* **2005**, *109*, 15422.
36. Lin, H.; Zhang, M.; Wang, F.; Meng, F.; Liao, B. Q.; Hong, H.; Chen, J.; Gao, W. *J. Membr. Sci.* **2014**, *460*, 110.
37. Rahimpour, A.; Madaeni, S. S.; Taheri, A. H.; Mansourpanah, Y. *J. Membr. Sci.* **2008**, *313*, 158.
38. Mendret, J.; Hatat-Fraile, M.; Rivallin, M.; Brosillon, S. *Sep. Purif. Technol.* **2013**, *111*, 9.
39. Shao, J.; Hou, J.; Song, H. *Water Res.* **2011**, *45*, 473.
40. Nguyen, T.; Roddick, F. A.; Fan, L. *Membranes* **2012**, *2*, 804.
41. Zhang, X.; Du, A. J.; Lee, P.; Sun, D. D.; Leckie, J. O. *J. Membr. Sci.* **2008**, *313*, 44.
42. Teow, Y. H.; Ahmad, A. L.; Lim, J. K.; Ooi, B. S. *Desalination* **2012**, *295*, 61.
43. Salgin, S.; Salgin, U.; Bahadir, S. *Int. J. Electrochem. Sci.* **2012**, *7*, 12404.
44. Zhang, G.; Ji, S.; Gao, X.; Liu, Z. *J. Membr. Sci.* **2008**, 309, *28*.